

The PqsE Active Site as a Target for Small Molecule Antimicrobial Agents against *Pseudomonas aeruginosa*

Isabelle R. Taylor, Philip D. Jeffrey, Dina A. Moustafa, Joanna B. Goldberg, and Bonnie L. Bassler*



Cite This: *Biochemistry* 2022, 61, 1894–1903



Read Online

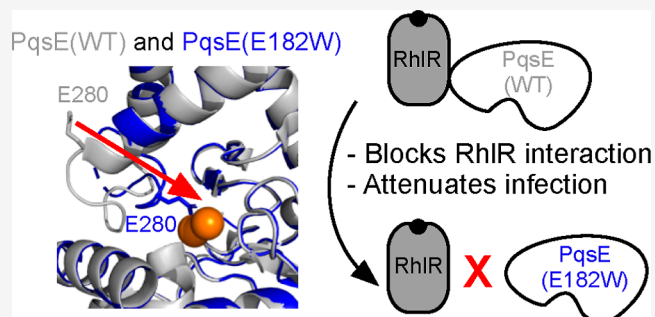
ACCESS |

Metrics & More

Article Recommendations

Supporting Information

ABSTRACT: The opportunistic pathogen *Pseudomonas aeruginosa* causes antibiotic-resistant, nosocomial infections in immunocompromised individuals and is a high priority for antimicrobial development. Key to pathogenicity in *P. aeruginosa* are biofilm formation and virulence factor production. Both traits are controlled by the cell-to-cell communication process called quorum sensing (QS). QS involves the synthesis, release, and population-wide detection of signal molecules called autoinducers. We previously reported that the activity of the RhlR QS transcription factor depends on a protein–protein interaction with the hydrolase, PqsE, and PqsE catalytic activity is dispensable for this interaction. Nonetheless, the PqsE–RhlR interaction could be disrupted by the substitution of an active site glutamate residue with tryptophan [PqsE(E182W)]. Here, we show that disruption of the PqsE–RhlR interaction via either the E182W change or alteration of PqsE surface residues that are essential for the interaction with RhlR attenuates *P. aeruginosa* infection in a murine host. We use crystallography to characterize the conformational changes induced by the PqsE(E182W) substitution to define the mechanism underlying disruption of the PqsE–RhlR interaction. A loop rearrangement that repositions the E280 residue in PqsE(E182W) is responsible for the loss of interaction. We verify the implications garnered from the PqsE(E182W) structure using mutagenic, biochemical, and additional structural analyses. We present the next generation of molecules targeting the PqsE active site, including a structure of the tightest binding of these compounds, BB584, in complex with PqsE. The findings presented here provide insights into drug discovery against *P. aeruginosa* with PqsE as the target.



INTRODUCTION

Pseudomonas aeruginosa is an opportunistic human pathogen that is responsible for untreatable infections in vulnerable, immunocompromised individuals.^{1,2} As a member of the “ESKAPE” multi-drug resistant pathogens, *P. aeruginosa* is a high-priority target for the development of next-generation antibiotics that function by new mechanisms of action.^{3,4} Features contributing to *P. aeruginosa* pathogenicity include the ability to produce virulence factors and to form biofilms.⁵ These traits are controlled by the bacterial cell–cell communication process called quorum sensing (QS).^{6–8}

QS involves the production, release, and population-wide detection and response to signal molecules called autoinducers.⁹ *P. aeruginosa* QS relies on two acyl-homoserine lactone (HSL) autoinducer production/detection systems, called Las and Rhl, and the Pqs alkyl quinolone autoinducer production/detection system.^{10–13} The Las system consists of the LasI autoinducer synthase and the LasR receptor/transcription factor which, respectively, produce and detect the autoinducer 3-oxo-C12-HSL.¹⁴ The Rhl system consists of the RhlI autoinducer synthase and the RhlR receptor/transcription factor, which, respectively, produce and detect the autoinducer C4-HSL¹⁵ (Figure 1a). The Pqs system

consists of the PQS autoinducer, synthesized by PqsABCD and PqsH, and its partner receptor/transcription factor, PqsR.^{16–19} The Las system sits at the top of the *P. aeruginosa* QS hierarchy and controls transcription of the components of the Rhl and Pqs systems.²⁰ Curiously, RhlR function additionally depends on the metallo- β -hydrolase enzyme PqsE, encoded as the final gene in the *pqsABCDE* biosynthetic operon.^{21–23} With respect to RhlR, PqsE is required to form a protein–protein interaction that enhances the affinity of RhlR for target promoters. PqsE catalytic activity is dispensable for this interaction and therefore is also not required for the production of pyocyanin and other RhlR-regulated virulence factors.^{24,25} Moreover, the RhlR–PqsE interaction is essential for *P. aeruginosa* virulence phenotypes, and therefore, of interest as a focus for antibiotic development.

Received: June 10, 2022

Revised: July 15, 2022

Published: August 19, 2022



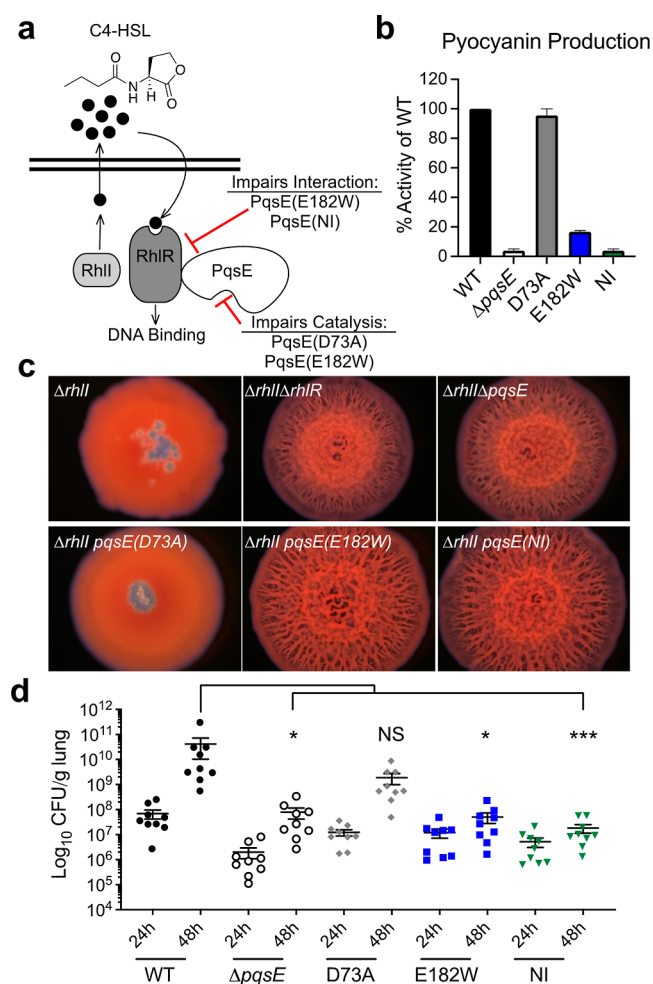


Figure 1. PqsE variants that are deficient in interaction with RhlR display attenuated pathogenicity. (a) The Rhl QS system in *P. aeruginosa*. See text for details. (b) Pyocyanin production by *P. aeruginosa* PA14 harboring the designated *pqsE* alleles at the native *pqsE* locus. The WT PA14 pyocyanin production level was set to 100%. Results are the average of two biological replicates. Error bars represent standard deviations. (c) Colony biofilm morphologies of the designated *P. aeruginosa* PA14 strains. Biofilms were imaged after 5 d of growth at 7.78 \times magnification. Images are representative of three biological replicates. (d) Lung colonization by the designated *P. aeruginosa* PA14, $\Delta pqsE$, *pqsE*(D73A), *pqsE*(E182W), or the *pqsE*(NI) strains in the murine infection model. Mice were euthanized at 24 and 48 h post-infection, and lung tissues were processed as described in [Materials/Experimental Details](#). All samples were plated for viable cfu on PIA. Each symbol represents the value for a single mouse. The data are pooled from two independent experiments. Error bars represent SEM. Statistical differences were determined using one-way ANOVA test and are as follows: ***, $P < 0.001$; *, $P < 0.05$; NS means not significant.

We recently showed that the ability of PqsE to interact with RhlR can be weakened by the introduction of an “inhibitor mimetic” mutation in which the glutamate residue at position 182 is altered to tryptophan [PqsE(E182W)].²⁴ The PqsE-(E182W) variant is a stable protein that, while harboring all of the catalytic residues, nonetheless displays less than 10% of wildtype catalytic activity, as if an inhibitor is bound in the active site. Residue E182 is buried deep within the active site of PqsE, at a location distant from the three surface arginine residues (R243, R246, and R247) that are necessary for PqsE to interact with RhlR. Mutation of the PqsE R243, R246, and

R247 residues to alanine completely abolishes the PqsE–RhlR interaction.²⁵ When introduced into *P. aeruginosa*, neither PqsE(E182W) nor PqsE(R243A/R246A/R247A) [the latter called PqsE(NI) for “non-interacting”] can promote PqsE–RhlR-dependent virulence phenotypes, including the production of the pyocyanin toxin. The effects of the PqsE E182W and PqsE NI substitutions on pyocyanin production are not through impairment of PqsE catalytic function, as the catalytically inactive variant, PqsE(D73A), remains fully capable of interacting with RhlR and driving pyocyanin production. These results indicate that PqsE has two independent functions, catalysis and interaction with RhlR, and it is interaction with RhlR, not catalysis, that is required for virulence.

From a drug discovery perspective, it is particularly promising that the PqsE active site E182W mutation weakens the distal PqsE–RhlR interaction, the consequence of which is the suppression of virulence phenotypes. We assert this because a PqsE active site-targeting molecule would likely be able to bind with high affinity and be more amenable to medicinal chemistry than a molecule targeting the interaction site on the surface of the protein. Protein–protein interactions, which typically occur over large, shallow protein surfaces, have proven notoriously difficult to target with small molecules.²⁶ Molecules that can bind in protein–protein interaction domains typically do so with weak affinity, are large and structurally complicated, and are difficult to optimize through medicinal chemistry efforts.²⁷ With this notion in mind, in this study, we aimed to determine the mechanism by which the PqsE E182W mutation disrupts the PqsE–RhlR interaction, and whether it is possible to achieve a similar effect with a small molecule inhibitor that binds in the PqsE active site. In a proof of principle experiment, we use our PqsE variants to demonstrate that disrupting the PqsE–RhlR interaction indeed attenuates in vivo *P. aeruginosa* virulence in a mouse lung infection model. We employ crystallography to characterize the structure of the PqsE(E182W) protein. We probe the functions of the PqsE active site through mutagenesis. Finally, we present the next generation of PqsE active site-targeting small molecules for further synthetic optimization. Our results can inform the discovery and/or design of effective antimicrobial agents to treat *P. aeruginosa* infections.

RESULTS

PqsE Variants that Cannot Interact with RhlR Display Attenuated Infection Phenotypes in Cell Assays and in a Mouse Lung Infection Model. We have shown previously that, unlike the overexpression of wildtype (WT) *pqsE*, the overexpression of *pqsE* mutants encoding proteins that cannot interact with RhlR in vitro impairs pyocyanin production in $\Delta pqsE$ *P. aeruginosa* PA14.^{24,25} To verify that the PqsE variants of interest display similar defects in virulence phenotypes when the genes encoding them are expressed from the native locus, we constructed *P. aeruginosa* PA14 strains harboring *pqsE*(D73A), *pqsE*(E182W), and *pqsE*(NI) on the chromosome. Western blots showed that the WT and variant PqsE proteins were produced at the same levels and exhibited similar stabilities (Figure S1). WT *P. aeruginosa* PA14 made pyocyanin while the $\Delta pqsE$ strain did not (4% compared to WT) (Figure 1b). When the PqsE variant proteins were produced from the chromosomally encoded genes, the results were entirely consistent with our previous findings for each PqsE variant produced from a plasmid. Specifically, the catalytically inactive

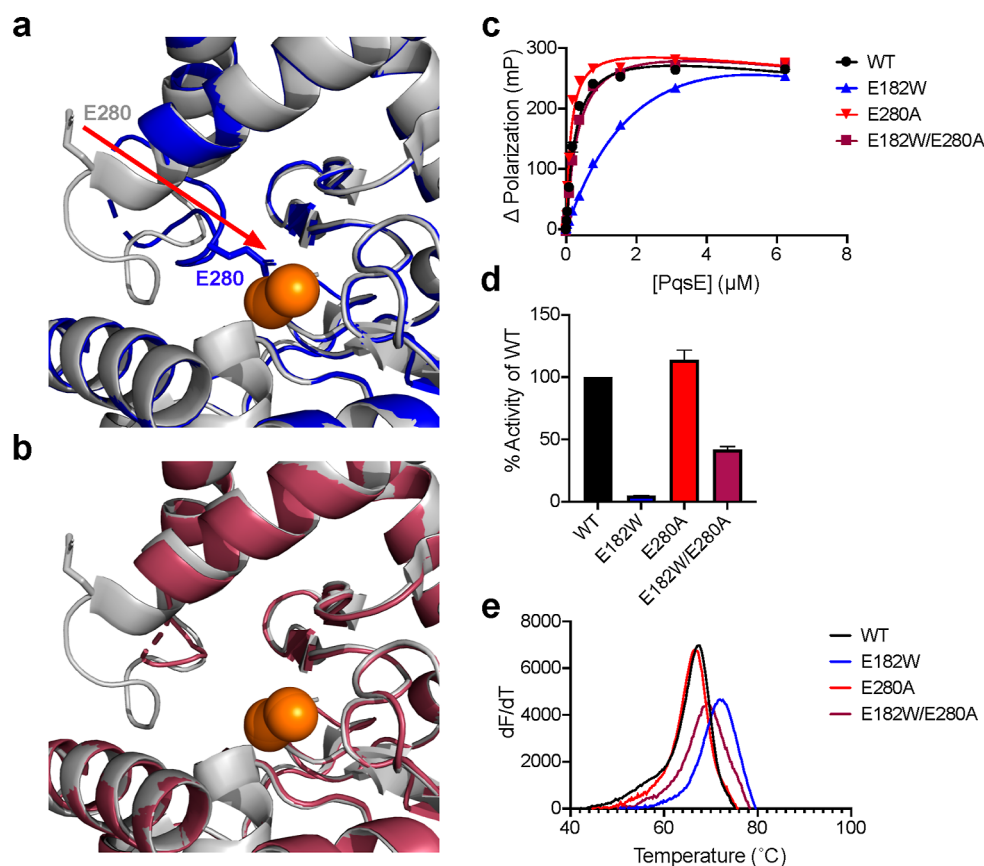


Figure 2. PqsE E182W substitution induces a loop rearrangement that repositions residue E280. (a) Structure of PqsE(E182W) (blue) overlaid with that of WT PqsE (PDB: 2Q0I, gray). The active site iron atoms are shown in orange. The red arrow indicates repositioning of E280 in PqsE(E182W) relative to its position in WT PqsE. (b) Structure of PqsE(E182W/E280A) (maroon) overlaid with that of WT PqsE (as in a). In panels a and b, residue E280 is shown in stick representation. (c) Binding of WT and variant PqsE proteins to the active site fluorescent probe BB562. K_{app} was determined in two independent experiments performed in triplicate. (d) Hydrolysis of 4-methylumbelliferyl butyrate (MUB) by the designated purified PqsE proteins. Values are represented as % activity of WT PqsE protein. Results are the average of two independent experiments performed in triplicate. Error bars represent standard deviations. (e) First derivative plots (dF/dT is defined as the change in SYPRO Orange fluorescence divided by change in temperature) of melting curves for the designated PqsE proteins. The peak of each curve is defined as the T_m of that protein.

PqsE(D73A) variant made nearly WT levels of pyocyanin (96%), the PqsE(E182W) inhibitor mimetic variant was severely impaired (17%), and the PqsE(NI) variant was incapable of driving pyocyanin production (4%) (Figure 1b).

Previously, we showed that the *P. aeruginosa* PA14 $\Delta rhII$ strain forms smooth colonies, whereas the $\Delta rhII \Delta rhIR$ and $\Delta rhII \Delta pqsE$ double mutants form biofilms with hyper-rugose morphologies.^{28,29} Thus, both PqsE and RhIR are required to suppress hyper-rugose biofilm formation in the absence of the C4-HSL autoinducer. To determine which specific function of PqsE, catalysis and/or interaction with RhIR, is linked to the control of biofilm morphology, we tested our PqsE variants. Each *pqsE* mutant was incorporated at the native chromosomal locus in the $\Delta rhII$ strain and biofilm morphology was assessed (Figure 1c). Both the $\Delta rhII pqsE(E182W)$ and $\Delta rhII pqsE(NI)$ mutants formed hyper-rugose biofilms similar to those of the $\Delta rhII \Delta rhIR$ and $\Delta rhII \Delta pqsE$ mutants. Only the $\Delta rhII$ strain harboring the *pqsE(D73A)* mutation exhibited the smooth biofilm morphology of the parent $\Delta rhII$ strain. This result demonstrates that the PqsE–RhIR interaction controls biofilm morphology and that PqsE catalytic activity is dispensable for this trait.

To explore the individual roles of PqsE catalysis and PqsE–RhIR interaction during host infection, we assessed the relative

pathogenicity of WT *P. aeruginosa* PA14, $\Delta pqsE$, *pqsE(D73A)*, *pqsE(E182W)*, and the *pqsE(NI)* strains in a murine model of acute pneumonia. Mice were infected intratracheally with equal strain inoculum levels ($\sim 3 \times 10^6$ cfu/mouse) and monitored over 48 h of infection. At 24 h, mice from all infection groups exhibited mild to moderate symptoms in response to infection, primarily displaying decreased mobility and increased breathing. Consistent with these symptoms, comparable levels of lung colonization were observed among all groups (Figure 1d). At 48 h, however, mice infected with either WT *P. aeruginosa* PA14 or the *pqsE(D73A)* mutant became more lethargic and appeared to progressively manifest additional symptoms, including increasingly labored breathing, hunched posture, and decreased response to stimuli. Moreover, those mice demonstrated >2 log increase in the bacterial burden compared to 24 h. In stark contrast, mice infected with the $\Delta pqsE$, *pqsE(E182W)*, or *pqsE(NI)* strains continued to display mild clinical symptoms with almost no change in their lung bacterial burden (Figure 1d). Together, the above findings demonstrate that the PqsE–RhIR interaction, and not PqsE catalytic activity, is responsible for shaping the pathogenicity of *P. aeruginosa* PA14 in vitro and in vivo.

PqsE E182W Substitution Induces a Loop Rearrangement near the Active Site. The above murine infection

experiment demonstrated that weakening the ability of PqsE to interact with RhlR by mutating an active site residue [PqsE(E182W)] causes a similarly severe reduction in infectivity to that caused by the complete elimination of the PqsE–RhlR interaction [PqsE(NI)]. To understand, at an atomic level, what conformational changes the E182W alteration induced in PqsE to affect its ability to interact with RhlR, we determined the structure of PqsE(E182W) (Figure 2a). Although the PqsE(E182W) crystals grow in the same $P3_221$ crystal form as WT PqsE, there is a significant structural rearrangement in the active site. In WT PqsE, the sidechain of E182 lies at the edge of the ligand binding site and makes hydrogen bonds with R191 and Q272. These interactions do not occur in PqsE(E182W), and rather, new interactions are made between the sidechain of the introduced W182 residue and F276, L277, and P278. The E182W change induces the rearrangement of the G270–L281 loop between helices 6 and 7, with a portion of that loop becoming disordered. Examination of electron density within the active site indicated a surprising consequence—with the sidechain of E280 relocating by 12 Å and becoming Fe bound in the center of the active site. Indeed, the repositioned E280 sidechain directly binds both Fe atoms, acting as a bridging ligand, and thus is most likely responsible for the stabilizing effect the E182W alteration has on PqsE, which we have reported previously.²⁴

To test whether repositioning of the PqsE E280 residue underpinned the inhibitor mimetic characteristics of the PqsE(E182W) protein, we engineered the E280A substitution into PqsE(E182W) to make PqsE(E182W/E280A). We determined the crystal structure of PqsE(E182W/E280A) revealing further changes in the PqsE active site. In this case, the presence of an alanine at residue 280 eliminated interaction with the iron atoms, and the loop consisting of residues D275–L281 was disordered (Figure 2b). The remainder of the loop was ordered and its structure reverted to a conformation that was more native-like than in PqsE(E182W). Consequently, the removal of the glutamate–Fe interaction via the E280A substitution apparently unblocked the active site of PqsE, partially restoring WT activity. Indeed, whereas PqsE(E182W) exhibits reduced binding affinity for the active site fluorescent probe, BB562, PqsE(E182W/E280A) displays WT binding affinity for the probe (Figure 2c). Furthermore, PqsE(E182W) has reduced hydrolytic capacity for a synthetic ester substrate, with only 7% activity relative to WT PqsE. The catalytic function of the PqsE(E182W/E280A) variant was greatly improved by the “unblocking” of the active site (34% compared to WT PqsE, Figure 2d). Consistent with the repositioning of E280 into the PqsE active site contributing to the increased stability of the PqsE(E182W) protein relative to WT PqsE, introduction of the E280A substitution reduced the T_m of the PqsE(E182W/E280A) protein to nearly that of WT PqsE (Figure 2e).

Introduction of the E280A alteration into PqsE(E182W) partially corrects the defects in small molecule binding and hydrolysis. Nonetheless, the PqsE(E182W/E280A) variant remains incapable of enhancing RhlR transcription factor activity in an *Escherichia coli* reporter assay and it does not drive pyocyanin production in *P. aeruginosa* PA14 (Figure 3a,b, respectively). Likewise, PqsE(E182W/E280A) is not improved for interaction with RhlR in vitro (Figure 4a). These findings further demonstrate the independence of the PqsE catalytic and virulence functions. Curiously, neither the PqsE(E182W)

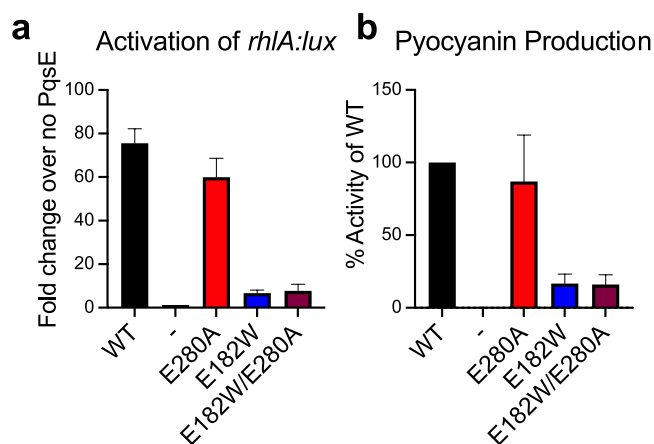


Figure 3. The PqsE E280A substitution does not restore the activation of RhlR transcriptional activity or pyocyanin production. (a) Light production from *E. coli* carrying P_{BAD} -*rhlR*, $PrhIA$ -*luxCDABE*, and the designated *pqsE* allele on the pACYC184 plasmid was measured following growth in the presence of 100 nM C4-HSL. The “-” symbol represents the strain carrying the empty pACYC184 vector. Results are the average of two biological replicates performed in technical triplicate. (b) Pyocyanin production was measured from $\Delta pqsE$ *P. aeruginosa* PA14 carrying the designated *pqsE* allele on the pUCP18 plasmid. The “-” symbol represents the strain carrying an empty pUCP18 plasmid. Results shown are the average of two biological replicates. Pyocyanin production from the strain with WT PqsE was set to 100%. Error bars represent standard deviations.

nor the PqsE(E182W/E280A) structure showed any changes in the region of the protein required for interaction with RhlR (R243, R246, and R247 on helix 5, Figure 2a,b, respectively). This result preliminarily suggests that either PqsE possesses an additional region of interaction with RhlR, perhaps employing the G270–L281 loop that is rearranged in PqsE(E182W) or partially disordered in PqsE(E182W/E280A), or alternatively, that a particular conformation of the G270–L281 loop is required to allosterically promote the interaction with RhlR. Irrespective of the underlying mechanism, the above structural and biochemical analyses characterizing PqsE(E182W) and PqsE(E182W/E280A) show that it is possible to disrupt the PqsE–RhlR interaction by manipulating the integrity of the G270–L281 loop that forms one face of the PqsE active site.

PqsE Variants Harboring Combinations of Substitutions Decouple Catalytic Activity from RhlR Interaction.

Our previous and above work comparing the inhibitor mimetic and RhlR non-interacting PqsE variants to the catalytically inactive PqsE(D73A) protein strongly suggest that the ability of PqsE to interact with RhlR and, in turn, drive virulence phenotypes is independent of PqsE enzyme activity. To confirm this notion, and, additionally, to explore the potential for influence of one activity on the other, we constructed PqsE variants containing combinations of amino acid substitutions underlying defects in enzyme activity, RhlR interaction, or both functions. Purity of these PqsE variant proteins was verified by SDS-PAGE analysis (Figure S2). We assessed the phenotypes of this set of variants in vitro, in recombinant *E. coli*, and in *P. aeruginosa* PA14. Specifically, we measured interaction of the purified PqsE variant proteins with RhlR by our pull-down assay (Figure 4a), intrinsic stability by T_m measurements (differential scanning fluorimetry, DSF), catalytic function by hydrolysis of the synthetic ester substrate MU-butyrate, and active site accessibility via binding of the

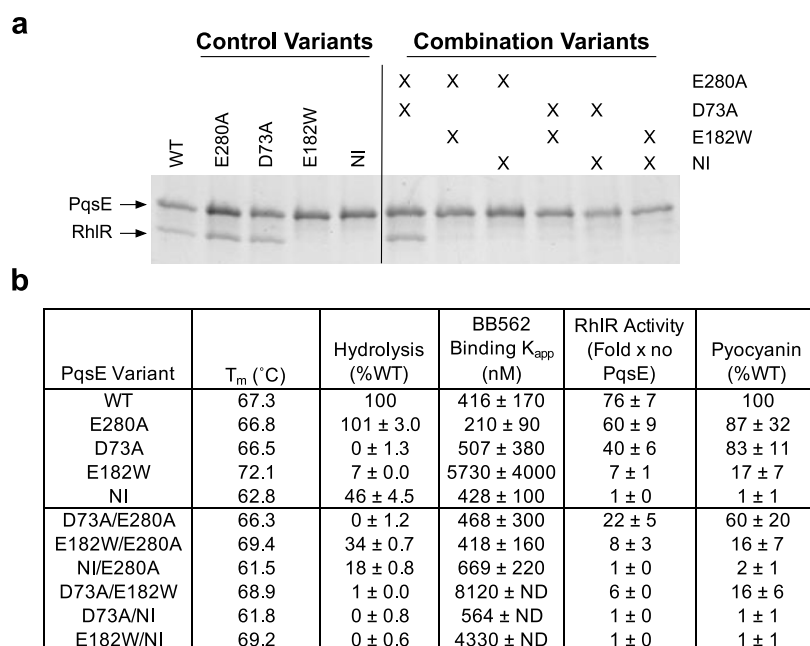


Figure 4. PqsE enzymatic activity is dispensable for RhlR interaction, RhlR transcriptional activity, and pyocyanin production. (a) Sodium dodecyl sulfate-polyacrylamide gel electrophoresis (SDS-PAGE) analysis of protein complexes formed in *in vitro* pull-down assays. 6xHis-PqsE proteins were immobilized on Ni resin and exposed to lysate containing RhlR. The resulting protein complexes were washed and eluted from the Ni resin and loaded into the lanes of the gel. PqsE appears as a ~34 kDa band and RhlR as a ~28 kDa band. For the variant combinations, “X” denotes that the protein in that lane contains the designated substitutions listed to the right. (b) Measured activities of PqsE variants in the designated assays. The full data from these analyses are provided in Figures S3 and S4 including replicate and statistical information. “ND” denotes that error could not be calculated for the binding curve, which occurred when the binding curve was too shallow or did not achieve saturation.

fluorescent active site probe, BB562 (Figure 4b). We measured the enhancement of RhlR transcriptional activity in the *E. coli* reporter assay and virulence by pyocyanin production in *P. aeruginosa* PA14 (Figure 4b). WT PqsE and the variants PqsE(E280A), PqsE(D73A), PqsE(E182W), and PqsE(NI) have all been previously characterized in this suite of assays and were included in our analyses for comparison to the variants containing combinations of substitutions. As shown in Figure 4 (and Figures S3 and S4), the ability of PqsE to form a complex with RhlR always tracked with the activation of RhlR transcription factor activity and pyocyanin production. By contrast, enzymatic capability did not correlate with the ability to form a complex with RhlR, activate RhlR transcription, or to produce pyocyanin.

One potential complication in the above analyses is that PqsE proteins harboring the “NI” triple arginine substitutions are less stable than WT and other of our variant PqsE proteins when overproduced in cells from a plasmid. Therefore, all variant proteins containing the NI substitutions were detected at lower levels compared to the other PqsE variant proteins in both *E. coli* and *P. aeruginosa* PA14 cell lysates (Figures S5 and S6). This feature could potentially have been the source of their apparent reduced activities in the RhlR transcriptional reporter assay and the pyocyanin assay. Our results with the PqsE(E182W/NI) variant show, however, that this is not the case. Due to the stabilizing effect of the E182W alteration (Figures 2 and S3), the PqsE(E182W/NI) protein was produced and detected at WT levels in both *E. coli* and *P. aeruginosa* lysates (Figures S5 and S6). Nonetheless, PqsE(E182W/NI) was completely inactive in both the pyocyanin production and RhlR transcriptional activity cell-based assays (Figure 3). This result confirms that the inability of select PqsE variants to activate RhlR and drive pyocyanin production stems

from loss of the PqsE–RhlR interaction, and is not the result of decreased PqsE protein production or stability.

Synthetic Optimization of an Active Site-targeting Small Molecule Scaffold. The results of our structural and mutagenic analyses suggest that manipulation of the PqsE active site, such that the G270–L281 loop becomes rearranged or disordered will result in decreased *P. aeruginosa* virulence due to inhibition of the PqsE–RhlR interaction. Thus, it is of interest to develop molecules that bind in the PqsE active site and, in so doing, inhibit the PqsE–RhlR interaction. We previously characterized two active site-targeting PqsE inhibitors, BB391 and BB393.²⁴ Crystallographic analyses of each compound bound to PqsE revealed their respective binding poses and interactions in the active site. Each inhibitor exhibited mid-nanomolar competition with the BB562 active site probe for binding to PqsE.²⁴

Guided by our crystal structures of BB391 and BB393 bound to PqsE, we designed a series of BB391–BB393 hybrid derivatives to probe the contributions of each moiety to binding affinity (Figure 5a). BB580 and BB581 were designed as the core hybrid structures, in which BB580 maintained the same amide bond orientation as in BB391, and BB581 possessed the amide bond orientation of BB393 (see position “1” in Figure 5a). BB580 outcompeted the BB562 probe with an EC_{50} of 99 nM compared to BB581 which exhibited an EC_{50} of 281 nM (Figure 5b,c). This result demonstrates that the preservation of the BB391 amide bond orientation coupled with the indazole ring, also from BB391, is superior for proper positioning of the carbonyl oxygen to form a hydrogen bond with PqsE residue S285. The structure of BB391 bound to PqsE showed that the possibility existed for π -stacking between the core phenyl ring and the H71 residue. Derivatives BB585, BB586, and BB589 were designed to test the enhancement of

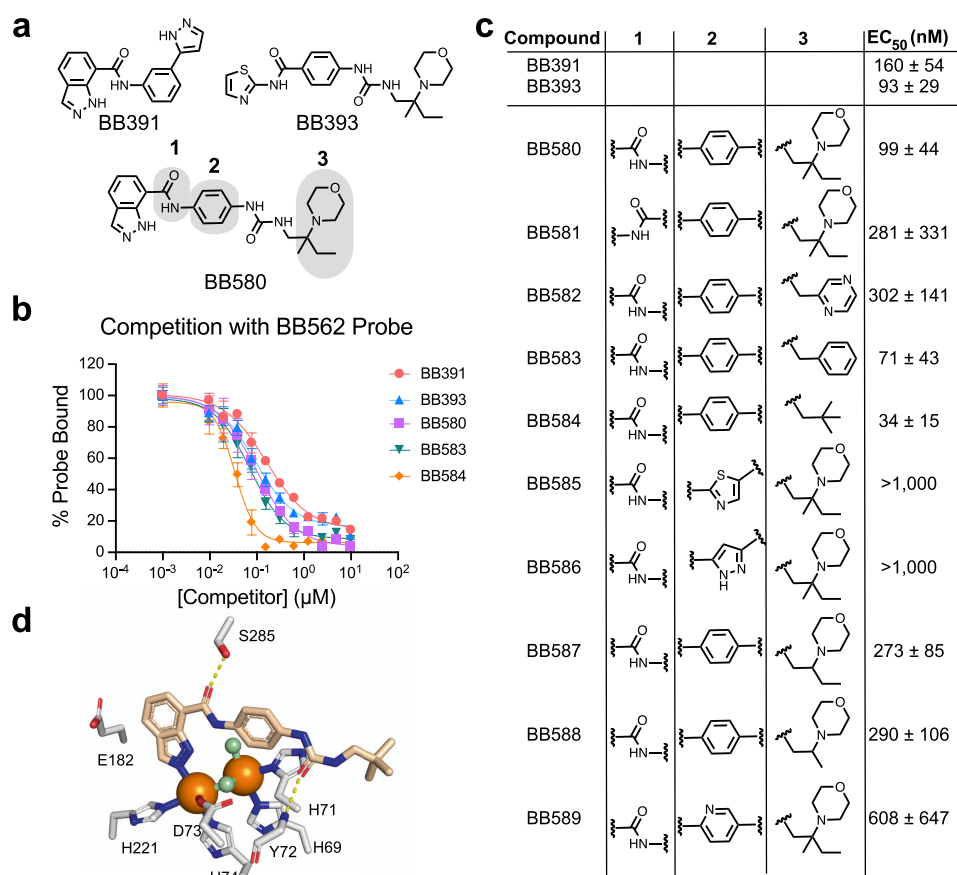


Figure 5. Optimization of new PqsE active site-targeting small molecules. (a) Structures of the precursor molecules BB391 and BB393 and the hybrid derivative BB580. Positions denoted 1, 2, and 3 were derivatized to explore the binding affinity for the PqsE active site. (b) Fluorescence polarization competition curves for select BB391–BB393 hybrid derivatives competing with the BB562 active site probe for binding to PqsE. Polarization value for PqsE–BB562 in the absence of a competitor is defined as 100% probe bound. All polarization values were background-subtracted by the reading for the probe in the absence of PqsE (background fluorescence). (c) Competitive fluorescence polarization EC₅₀ values calculated for all BB391–BB393 derivatives, determined from one experiment performed in triplicate. (d) Structure of BB584 bound to PqsE. Both the BB584 molecule and key PqsE amino acid sidechains are shown as sticks. Amino acid sidechain carbons are depicted in gray and BB584 carbons are shown in tan. Iron atoms and water molecules are shown as orange and green spheres, respectively. Oxygen and nitrogen atoms are in red and blue, respectively. Hydrogen bonds are shown as dotted yellow lines.

π -stacking with alternative aromatic groups at this core position (see position “2” in Figure 5a). None of these three derivatives, featuring thiazole, pyrazole, or pyridine rings, respectively, bound as tightly as BB580, and therefore among the molecules tested, a phenyl ring was deemed ideal at this core position (Figure 5b,c). Finally, derivatives BB582, BB583, BB584, BB587, and BB588 were designed to assess the importance of a hydrophobic moiety on the BB393 molecule (see position “3” in Figure 5a), which in the crystal structure, nestles into a hydrophobic groove near the solvent-exposed entrance to the PqsE active site. The results with BB587 and BB588 show that elimination of either the methyl or ethyl groups, respectively, leads to slightly decreased binding affinity (EC₅₀ = 273 and 290 nM, respectively). However, if the morpholine ring is removed and either a phenyl (BB583) or *tert*-butyl (BB584) group is installed, a modest increase in binding affinity is achieved (EC₅₀ = 71 and 34 nM, respectively) (Figure 5b,c). Such improvement was not observed for BB582, featuring a pyrazine ring, suggesting that increased hydrophobicity of this portion of the molecule tracks with the increased engagement of the hydrophobic groove in PqsE. None of the derivatives described here inhibit the PqsE–RhIR interaction. Within that context, BB584

displayed the tightest binding to PqsE and provides a starting scaffold for the design of new derivatives.

We determined the crystal structure of BB584 bound to PqsE, which showed a similar orientation in the active site and similar ligand–protein interactions to those observed in the crystal structures of PqsE with BB391 and BB393 bound in the active site (Figure 5d). Specifically, the nitrogen on the indazole ring of BB584 bonds with the Fe2 atom, displacing a water molecule that normally resides at this position. Two additional hydrogen bonds exist between BB584 and PqsE sidechains: the BB584 amide oxygen with the hydroxyl group of the S285 sidechain, and the BB584 urea oxygen with the backbone amide N–H of residue Y72. As predicted, the *tert*-butyl group tucks into the hydrophobic groove that sits between the α -helix consisting of PqsE residues S104–L116 and the backbone of the conserved ⁶⁹HXHXDH⁷⁴ motif. Analogous to the structures of BB391 and BB393 bound to PqsE, no significant conformational changes in the protein were induced by binding of BB584 (rmsd of 0.24 Å for 293 C α atoms), possibly explaining why none of the three compounds disrupt the PqsE–RhIR interaction. Nonetheless, the structures of these ligands bound to WT PqsE along with the structures of PqsE(E182W) and PqsE(E182W/E280A) can be

used as guides in the design of new derivatives with the potential to disrupt the interaction between PqsE and RhlR.

MATERIALS/EXPERIMENTAL DETAILS

Strains, Media, and Molecular Procedures. The *P. aeruginosa* UCBPP-PA14 strain was used as the parental strain for all experiments involving *P. aeruginosa*. All strains were grown in Luria–Bertani broth, unless otherwise stated, and antibiotics were used at the following concentrations: ampicillin (200 $\mu\text{g}/\text{mL}$), kanamycin (100 $\mu\text{g}/\text{mL}$), tetracycline (10 $\mu\text{g}/\text{mL}$), carbenicillin (400 $\mu\text{g}/\text{mL}$), gentamycin (30 $\mu\text{g}/\text{mL}$), and irgasan (100 $\mu\text{g}/\text{mL}$). Plasmids were constructed following a previously reported site-directed mutagenesis protocol³⁰ and were transformed into *P. aeruginosa* PA14 strains as described.³¹ Deletion of and point mutations in *pqsE* were generated by a previously reported method, with some modifications.²⁸ Briefly, *pqsE* variants were cloned onto the pEXG2 vector. *E. coli* SM10 λ pir carrying each pEXG2-*pqsE*-containing plasmid was mated with *P. aeruginosa* PA14 or the Δ rhlI strain and exconjugants were selected on LB agar containing gentamycin and irgasan. Colonies were grown in LB medium at 37 °C for 1–2 h and plated on LB agar containing 5% sucrose to force the elimination of the *sacB* gene on the plasmid. Resulting colonies were patched onto LB agar plates and onto plates containing gentamycin, and *pqsE* variants in Gent^s colonies were confirmed by sequencing. Strains used in this study are listed in Supporting Information, Table S1.

General Methods. 6xHis-PqsE proteins were purified for biochemical assays (tagged) and crystallography (tag removed), as described previously.²⁴ Enzyme activities of purified 6xHis-PqsE variants were measured as previously reported with MU-butyrate as the substrate.²⁵ Fluorescence polarization assays with the BB562 active site probe were performed as described.²⁴ The melting temperature (T_m) of each purified 6xHis-PqsE variant was measured using DSF as described previously.²⁴ Interaction between PqsE and RhlR proteins in vitro was measured as described previously using pull-down assays.²⁴ Pyocyanin production by *P. aeruginosa* PA14 strains carrying *pqsE* variants on the pUCP18 plasmid was measured as described.²⁴ The ability of PqsE variants to increase RhlR transcription factor activity in an *E. coli* reporter assay was assessed as previously described.²⁴ All small molecule syntheses and characterization are described in the Supporting Information.

Colony Biofilm Morphology Assay. Cultures were grown overnight in LB broth with shaking at 37 °C, and 1 μL of culture was spotted onto a 60 \times 15 mm Petri plate containing 10 mL of biofilm medium (1% Tryptone, 1% agar, 40 mg/L Congo Red, 20 mg/L Coomassie Brilliant Blue). Biofilms were grown at 25 °C for several days and imaged throughout their development on a Leica stereomicroscope M125 mounted with a Leica MC170 HD camera at 7.78 \times magnification.

Mouse Lung Infection Studies. For all mouse experiments, *P. aeruginosa* strains were grown on *Pseudomonas* Isolation Agar (PIA) for 16–18 h at 37 °C and suspended in PBS to an OD₆₀₀ of 0.5, corresponding to $\sim 10^9$ cfu/mL. These samples were adjusted spectrophotometrically and then diluted to the appropriate OD₆₀₀ in phosphate-buffered saline (PBS). Eight-to-ten-week-old female BALB/c mice (Jackson Laboratories, Bar Harbor, ME) were anesthetized by the intraperitoneal injection of 0.2 mL of a mixture of ketamine (25 mg/mL) and xylazine (12 mg/mL). Mice were infected by

noninvasive intratracheal instillation³² of 50 μL of $\sim 3 \times 10^6$ cfu of *P. aeruginosa* WT or isogenic mutants. Mice were euthanized at 24 and 48 h post-infection and whole lungs were collected aseptically, weighed, and homogenized in 1 mL of PBS. Bacterial loads in tissue homogenates were enumerated by serial dilution and plating on PIA. Comparison and analyses of the numbers of viable bacteria obtained in lung homogenates were performed using GraphPad Prism version 7 software. Results were analyzed using one-way analysis of variance (ANOVA) and were compared using the Kruskal–Wallis test for comparison of three groups or the Mann–Whitney *U* test for the analysis of two groups.

Protein Crystallography. Purified proteins (~ 10 mg/mL) and protein–compound complexes were crystallized by hanging drop vapor diffusion at 22 °C following mixing at a 1:1 ratio with the well buffer. Crystallization buffers used were as follows: PqsE(E182W) (0.1 M HEPES pH 7.5, 0.2 M MgCl₂, 15% (w/v) PEG 400) cryoprotected with 20% (v/v) glycerol prior to freezing, PqsE(E182W/E280A) (0.1 M HEPES pH 7.5, 0.2 M MgCl₂, 27% (w/v) PEG 400) cryoprotected with 10% (v/v) ethylene glycol prior to freezing, and PqsE-BB584 (0.1 M HEPES pH 7.5, 0.2 M MgCl₂, 15% (v/v) 2-propanol) cryoprotected with 30% (v/v) ethylene glycol with additional BB584 (50 μM) in the cryoprotectant solution. Crystals typically formed within 48 h, but in some cases, took up to 5 days to form. PqsE(E182W), PqsE(E182W/E280A), and PqsE-BB584 crystals each grew in the same trigonal space group as had been previously observed for WT PqsE, PqsE-BB391, and PqsE-BB393 ($P3_221$, $a = b = 60$ Å $c = 146$ Å $\alpha = \beta = 90^\circ$, $\gamma = 120^\circ$) with one molecule in the asymmetric unit. Data were collected on either the 17-ID-1 beamline of the NSLS-II synchrotron [PqsE(E182W) and PqsE(E182W/E280A)], or on a Rigaku MicroMax 007HF rotating anode source (PqsE-BB584) (Table S2). Data were processed either with XDS³³ and AIMLESS³⁴ or with DENZO and SCALEPACK.³⁵ The starting model for each refinement was a prior ligand-bound structure (7KGX²⁴) with the ligand and water molecules removed but the iron atoms retained, subjected to rigid-body refinement, followed by conventional refinement using Phenix.refine.³⁶ The structures were iteratively rebuilt using Coot³⁷ and refined with Phenix.refine. Both PqsE variant proteins exhibited significant conformational changes in a loop region (G270–L281) relative to the starting model, which remodeled the active site. In the case of the BB584 ligand, an atomic model of the ligand was fit to the difference electron density observed in the active site of PqsE and refined with partial occupancy (0.93). Final refinement statistics are shown in Table S2 including the identifiers for the structures' depositions in the Protein Data Bank [PqsE-(E182W) PDB ID: 7TZ9, PqsE(E182W/E280A): 7U6G, and PqsE-BB584 PDB ID: 7TZA].

CONCLUSIONS

PqsE has two biochemical activities, a protein–protein interaction with RhlR, which increases RhlR transcriptional activity at target promoters, and an esterase activity. The substrate and product of PqsE catalysis are currently unknown and ongoing research aims to identify them. Here, we showed that the PqsE–RhlR interaction is separable from the PqsE catalytic activity. Moreover, we engineered a set of PqsE variant proteins that possess every combination of the two activities (catalytic⁺/interaction⁺, catalytic⁻/interaction⁺, catalytic⁺/interaction⁻, and catalytic⁻/interaction⁻). Analysis of

these proteins, coupled with previous work, shows that the PqsE–RhIR interaction is linked to virulence factor production in *P. aeruginosa* PA14. Here, we demonstrated that the PqsE–RhIR interaction also controls the development of *P. aeruginosa* PA14 biofilm morphology and is crucial for establishing an infection in a host animal. Remarkably, PqsE catalytic function is dispensable for the regulation of RhIR-transcriptional activity, biofilm morphology, virulence factor production, and animal infectivity. As the PqsE variant phenotypes are consistent between all assays performed, the set of cell-based assays we employ here can effectively be used in lieu of infectivity assays in animals to probe and predict the potential of small molecules as *P. aeruginosa* antibiotics that target PqsE.

Our finding that the PqsE–RhIR interaction was disrupted following the introduction of the E182W substitution in the PqsE active site was surprising given that this residue is distal to the RhIR interaction site.²⁵ The crystal structure of PqsE(E182W) revealed that a loop rearrangement inserts the E280 residue into the active site to coordinate both of the iron atoms at this site. It is the repositioning of E280 in the PqsE(E182W) variant—blocking substrate access to the catalytic iron atoms—that is responsible for the “inhibitor mimic” nature of this variant. Catalytic activity is restored in the PqsE(E182W/E280A) variant because the alanine substitution clears the active site, thus enabling substrate binding; however, PqsE(E182W/E280A) remains incapable of interacting with RhIR (Figures 3 and 4). Analysis of the PqsE(E182W/E280A) structure, and the surprisingly modest conformational changes that are apparent compared to the structures of WT PqsE and PqsE(E182W) (Figure 2a,b), suggest that the structural integrity of the G270–L281 loop is essential for PqsE to interact with RhIR. These results confirm that, although the RhIR-interaction is independent of PqsE catalytic activity, structural changes induced through the active site of PqsE can disrupt interaction with RhIR.

All prior crystal structures of WT PqsE showed that the E280 residue resides on the surface with the glutamate sidechain directed outward into the solvent. Our data show that single substitution of this glutamate with alanine [i.e., PqsE(E280A)] increased accessibility of the PqsE active site (Figure 2c). This finding potentially points to naturally occurring PqsE conformational dynamics in which the position of the E280 sidechain alternates between facing the solvent and being inserted into the active site. While not proven, it is possible that E280 serves as a dynamic gate-keeper residue for the active site. Perhaps, its position determines whether PqsE will undergo catalysis and/or will interact with RhIR. Such a mechanism would make considerations of the PqsE E280 sidechain position key for future drug discovery efforts.³⁸ We recognize that our proposed ideas for how positioning of the PqsE E280 residue influences interaction with RhIR are speculative. Additional experimental investigation is required to reveal whether PqsE undergoes natural conformational dynamics that influence its interactions with RhIR and whether structural flexibility plays any role in its putative enzyme function.

Figure 5 presents a new series of molecules, inspired by the previous PqsE inhibitors BB391 and BB393, all of which bind in the PqsE active site. Our competitive binding assay allowed us to rank derivatives by their relative affinities providing preliminary structure–activity relationships (SAR). The molecules presented here were derivatized at positions that do not contact the regions of the PqsE active site at which the

E182W substitution perturbs the structure. Thus, it is not surprising that the compounds do not affect the PqsE–RhIR interaction. Rather, the SAR explored in the current compound series was designed to probe interactions of the small molecule scaffolds with two regions of the active site: the iron-binding site and the hydrophobic groove near the solvent-exposed face of the active site. This compound series enabled identification of high-affinity PqsE active site binders that can be further derivatized, potentially at the indazole ring, to allosterically inhibit the interaction with RhIR. Among this set, compound BB584 binds most tightly in the PqsE active site ($EC_{50} = 34$ nM). The crystal structure of the PqsE–BB584 complex solved here (Figure 5c) provides needed information for launching the structure-guided design of the next generation of molecules targeting the PqsE active site. An alternative strategy afforded by these molecules would be their use in proteolysis targeting chimera (PROTAC) design with PqsE as the target. Indeed, recent developments focused on using PROTACs for the targeted degradation of bacterial proteins encourage the use of such high-affinity ligands for this purpose.³⁹ Our PqsE variant analyses and companion structures should propel the design of high affinity active site-targeting compounds that do disrupt the PqsE–RhIR interaction via an allosteric mechanism, presumably involving the movement of the G270–L281 loop.

ETHICS STATEMENT

All mouse procedures were performed in accordance with the established guidelines of the Emory University Institutional Animal Care and Use Committee (IACUC) under protocol number DAR-201700441. This study was carried out in strict accordance with established guidelines and policies at Emory University School of Medicine, the recommendations in the Guide for Care and Use of Laboratory Animals,⁴⁰ as well as local, state, and federal laws.

ASSOCIATED CONTENT

Supporting Information

The Supporting Information is available free of charge at <https://pubs.acs.org/doi/10.1021/acs.biochem.2c00334>.

Western blot characterization of PqsE proteins from cell lysates, SDS-PAGE analysis and biochemical characterization of purified PqsE variants, in vivo characterization of PqsE variants, SAR for BB391–BB393 hybrid derivatives, strains used in this study, crystallographic data collection and refinement statistics, and detailed synthetic methods (PDF)

Accession Codes

PqsE: A0A0H2Z6F6. RhIR: A0A0H2ZEG8.

AUTHOR INFORMATION

Corresponding Author

Bonnie L. Bassler — Department of Molecular Biology, Princeton University, Princeton, New Jersey 08544, United States; Howard Hughes Medical Institute, Chevy Chase, Maryland 20815, United States; orcid.org/0000-0002-0043-746X; Email: bbassler@princeton.edu

Authors

Isabelle R. Taylor — Department of Molecular Biology, Princeton University, Princeton, New Jersey 08544, United States; orcid.org/0000-0003-1053-5677

Philip D. Jeffrey – Department of Molecular Biology, Princeton University, Princeton, New Jersey 08544, United States

Dina A. Moustafa – School of Medicine, Children's Healthcare of Atlanta, Inc., Department of Pediatrics, and Center for Cystic Fibrosis and Airway Diseases Research, Emory University, Atlanta, Georgia 30322, United States

Joanna B. Goldberg – School of Medicine, Children's Healthcare of Atlanta, Inc., Department of Pediatrics, and Center for Cystic Fibrosis and Airway Diseases Research, Emory University, Atlanta, Georgia 30322, United States

Complete contact information is available at:

<https://pubs.acs.org/10.1021/acs.biochem.2c00334>

Author Contributions

I.R.T., P.D.J., and D.A.M. conducted experiments; I.R.T., P.D.J., D.A.M., J.B.G., and B.L.B. designed experiments and prepared the manuscript.

Notes

The authors declare no competing financial interest.

ACKNOWLEDGMENTS

We thank members of the Bassler laboratory for helpful advice and discussions. We are grateful to William Miller and Brad Henke for guidance in chemical strategies and synthetic procedures. Molecules used in this study were synthesized at WuXi AppTec. Protein crystallography was performed in the Macromolecular Crystallography Core Facility at Princeton University. The AMX beamline of the National Synchrotron Light Source II, a U.S. Department of Energy (DOE) Office of Science User Facility operated for the DOE Office of Science by Brookhaven National Laboratory was also used under Contract DE-SC0012704. This work was supported by the Howard Hughes Medical Institute, NIH grant 2R37GM065859, and National Science Foundation grant MCB-2043238 to B.L.B., and NIH grant F32GM134583 to I.R.T. The content herein is solely the responsibility of the authors and does not represent the official views of the National Institutes of Health. The authors declare that they have no competing financial interest.

REFERENCES

- (1) Driscoll, J. A.; Brody, S. L.; Kollef, M. H. The Epidemiology, Pathogenesis and Treatment of *Pseudomonas Aeruginosa* Infections. *Drugs* **2007**, *67*, 351–368.
- (2) Kang, C.-I.; Kim, S.-H.; Kim, H.-B.; Park, S.-W.; Choe, Y.-J.; Oh, M.-D.; Kim, E.-C.; Choe, K.-W. *Pseudomonas aeruginosa* Bacteremia: Risk Factors for Mortality and Influence of Delayed Receipt of Effective Antimicrobial Therapy on Clinical Outcome. *Clin. Infect. Dis.* **2003**, *37*, 745–751.
- (3) Breidenstein, E. B. M.; de la Fuente-Núñez, C.; Hancock, R. E. W. *Pseudomonas Aeruginosa*: All Roads Lead to Resistance. *Trends Microbiol.* **2011**, *19*, 419–426.
- (4) De Oliveira, D. M. P.; Forde, B. M.; Kidd, T. J.; Harris, P. N. A.; Schembri, M. A.; Beatson, S. A.; Paterson, D. L.; Walker, M. J. Antimicrobial Resistance in ESKAPE Pathogens. *Clin. Microbiol. Rev.* **2020**, *33*, No. e00181.
- (5) Moradali, M. F.; Ghods, S.; Rehm, B. H. A. *Pseudomonas Aeruginosa* Lifestyle: A Paradigm for Adaptation, Survival, and Persistence. *Front. Cell. Infect. Microbiol.* **2017**, *7*, 39.
- (6) Chadha, J.; Harjai, K.; Chhibber, S. Revisiting the Virulence Hallmarks of *Pseudomonas Aeruginosa*: A Chronicle through the Perspective of Quorum Sensing. *Environ. Microbiol.* **2021**, *24*, 2630.
- (7) O'Loughlin, C. T.; Miller, L. C.; Siryaporn, A.; Drescher, K.; Semmelhack, M. F.; Bassler, B. L. A Quorum-Sensing Inhibitor Blocks *Pseudomonas Aeruginosa* Virulence and Biofilm Formation. *Proc. Natl. Acad. Sci. U.S.A.* **2013**, *110*, 17981.
- (8) Flickinger, S. T.; Copeland, M. F.; Downes, E. M.; Braasch, A. T.; Tuson, H. H.; Eun, Y.-J.; Weibel, D. B. Quorum Sensing between *Pseudomonas Aeruginosa* Biofilms Accelerates Cell Growth. *J. Am. Chem. Soc.* **2011**, *133*, 5966–5975.
- (9) Rutherford, S. T.; Bassler, B. L. Bacterial Quorum Sensing: Its Role in Virulence and Possibilities for Its Control. *Cold Spring Harbor Perspect. Med.* **2012**, *2*, a012427.
- (10) Passador, L.; Cook, J. M.; Gambello, M. J.; Rust, L.; Iglewski, B. H. Expression of *Pseudomonas Aeruginosa* Virulence Genes Requires Cell-to-Cell Communication. *Science* **1993**, *260*, 1127–1130.
- (11) Heeb, S.; Fletcher, M. P.; Chhabra, S. R.; Diggle, S. P.; Williams, P.; Cámara, M. Quinolones: From Antibiotics to Auto-inducers. *FEMS Microbiol. Rev.* **2011**, *35*, 247–274.
- (12) Pesci, E. C.; Milbank, J. B.; Pearson, J. P.; McKnight, S.; Kende, A. S.; Greenberg, E. P.; Iglewski, B. H. Quinolone Signaling in the Cell-to-Cell Communication System of *Pseudomonas Aeruginosa*. *Proc. Natl. Acad. Sci. U.S.A.* **1999**, *96*, 11229–11234.
- (13) Welsh, M. A.; Eibergen, N. R.; Moore, J. D.; Blackwell, H. E. Small Molecule Disruption of Quorum Sensing Cross-Regulation in *Pseudomonas Aeruginosa* Causes Major and Unexpected Alterations to Virulence Phenotypes. *J. Am. Chem. Soc.* **2015**, *137*, 1510–1519.
- (14) Pearson, J. P.; Gray, K. M.; Passador, L.; Tucker, K. D.; Eberhard, A.; Iglewski, B. H.; Greenberg, E. P. Structure of the Autoinducer Required for Expression of *Pseudomonas Aeruginosa* Virulence Genes. *Proc. Natl. Acad. Sci. U.S.A.* **1994**, *91*, 197–201.
- (15) Pearson, J. P.; Passador, L.; Iglewski, B. H.; Greenberg, E. P. A Second N-Acylhomoserine Lactone Signal Produced by *Pseudomonas Aeruginosa*. *Proc. Natl. Acad. Sci. U.S.A.* **1995**, *92*, 1490–1494.
- (16) Rampioni, G.; Falcone, M.; Heeb, S.; Frangipani, E.; Fletcher, M. P.; Dubern, J.-F.; Visca, P.; Leoni, L.; Cámara, M.; Williams, P. Unravelling the Genome-Wide Contributions of Specific 2-Alkyl-4-Quinolones and PqsE to Quorum Sensing in *Pseudomonas Aeruginosa*. *PLoS Pathog.* **2016**, *12*, No. e1006029.
- (17) Drees, S. L.; Fetzner, S. PqsE of *Pseudomonas Aeruginosa* Acts as Pathway-Specific Thioesterase in the Biosynthesis of Alkylquinolone Signaling Molecules. *Chem. Biol.* **2015**, *22*, 611–618.
- (18) Storz, M. P.; Maurer, C. K.; Zimmer, C.; Wagner, N.; Brengel, C.; de Jong, J. C.; Lucas, S.; Müsken, M.; Häußler, S.; Steinbach, A.; Hartmann, R. W. Validation of PqsD as an Anti-Biofilm Target in *Pseudomonas Aeruginosa* by Development of Small-Molecule Inhibitors. *J. Am. Chem. Soc.* **2012**, *134*, 16143–16146.
- (19) Prothiwa, M.; Englmaier, F.; Böttcher, T. Competitive Live-Cell Profiling Strategy for Discovering Inhibitors of the Quinolone Biosynthesis of *Pseudomonas Aeruginosa*. *J. Am. Chem. Soc.* **2018**, *140*, 14019–14023.
- (20) Lee, J.; Zhang, L. The Hierarchy Quorum Sensing Network in *Pseudomonas Aeruginosa*. *Protein Cell* **2015**, *6*, 26–41.
- (21) Farrow, J. M.; Sund, Z. M.; Ellison, M. L.; Wade, D. S.; Coleman, J. P.; Pesci, E. C. PqsE Functions Independently of PqsR-*Pseudomonas* Quinolone Signal and Enhances the rhl Quorum-Sensing System. *J. Bacteriol.* **2008**, *190*, 7043–7051.
- (22) Groleau, M.-C.; de Oliveira Pereira, T.; Dekimpe, V.; Déziel, E. PqsE Is Essential for RhlR-Dependent Quorum Sensing Regulation in *Pseudomonas Aeruginosa*. *mSystems* **2020**, *5*, No. e00194.
- (23) Zender, M.; Witzgall, F.; Drees, S. L.; Weidel, E.; Maurer, C. K.; Fetzner, S.; Blankenfeldt, W.; Empting, M.; Hartmann, R. W. Dissecting the Multiple Roles of PqsE in *Pseudomonas Aeruginosa* Virulence by Discovery of Small Tool Compounds. *ACS Chem. Biol.* **2016**, *11*, 1755–1763.
- (24) Taylor, I. R.; Paczkowski, J. E.; Jeffrey, P. D.; Henke, B. R.; Smith, C. D.; Bassler, B. L. Inhibitor Mimetic Mutations in the *Pseudomonas Aeruginosa* PqsE Enzyme Reveal a Protein-Protein Interaction with the Quorum-Sensing Receptor RhlR That Is Vital for Virulence Factor Production. *ACS Chem. Biol.* **2021**, *16*, 740–752.

(25) Simanek, K. A.; Taylor, I. R.; Richael, E. K.; Lasek-Nesselquist, E.; Bassler, B. L.; Paczkowski, J. E. The PqsE-RhIR Interaction Regulates RhIR DNA Binding to Control Virulence Factor Production in *Pseudomonas Aeruginosa*. *Microbiol. Spectr.* **2022**, *10*, No. e0210821.

(26) Cesa, L. C.; Mapp, A. K.; Gestwicki, J. E. Direct and Propagated Effects of Small Molecules on Protein-Protein Interaction Networks. *Front. Bioeng. Biotechnol.* **2015**, *3*, 119.

(27) Ran, X.; Gestwicki, J. E. Inhibitors of Protein-Protein Interactions (PPIs): An Analysis of Scaffold Choices and Buried Surface Area. *Curr. Opin. Chem. Biol.* **2018**, *44*, 75–86.

(28) Mukherjee, S.; Moustafa, D.; Smith, C. D.; Goldberg, J. B.; Bassler, B. L. The RhIR Quorum-Sensing Receptor Controls *Pseudomonas Aeruginosa* Pathogenesis and Biofilm Development Independently of Its Canonical Homoserine Lactone Autoinducer. *PLoS Pathog.* **2017**, *13*, No. e1006504.

(29) Mukherjee, S.; Moustafa, D. A.; Stergioula, V.; Smith, C. D.; Goldberg, J. B.; Bassler, B. L. The PqsE and RhIR Proteins Are an Autoinducer Synthase–Receptor Pair That Control Virulence and Biofilm Development in *Pseudomonas Aeruginosa*. *Proc. Natl. Acad. Sci. U.S.A.* **2018**, *115*, No. E9411.

(30) McCready, A. R.; Paczkowski, J. E.; Henke, B. R.; Bassler, B. L. Structural Determinants Driving Homoserine Lactone Ligand Selection in the *Pseudomonas Aeruginosa* LasR Quorum-Sensing Receptor. *Proc. Natl. Acad. Sci. U.S.A.* **2019**, *116*, 245.

(31) Choi, K.-H.; Kumar, A.; Schweizer, H. P. A 10-Min Method for Preparation of Highly Electrocompetent *Pseudomonas Aeruginosa* Cells: Application for DNA Fragment Transfer between Chromosomes and Plasmid Transformation. *J. Microbiol. Methods* **2006**, *64*, 391–397.

(32) Revelli, D. A.; Boylan, J. A.; Gherardini, F. C. A Non-Invasive Intratracheal Inoculation Method for the Study of Pulmonary Melioidosis. *Front. Cell. Infect. Microbiol.* **2012**, *2*, 164.

(33) Kabsch, W. XDS. *Acta Crystallogr., Sect. D: Biol. Crystallogr.* **2010**, *66*, 125–132.

(34) Evans, P. R.; Murshudov, G. N. How Good Are My Data and What Is the Resolution? *Acta Crystallogr., Sect. D: Biol. Crystallogr.* **2013**, *69*, 1204.

(35) Otwinowski, Z.; Minor, W. Denzo and Scalepack. *Int. Tables Crystallogr.* **2001**, *276*, 226–235.

(36) Liebschner, D.; Afonine, P. V.; Baker, M. L.; Bunkóczi, G.; Chen, V. B.; Croll, T. I.; Hintze, B.; Hung, L. W.; Jain, S.; McCoy, A. J.; Moriarty, N. W.; Oeffner, R. D.; Poon, B. K.; Prisant, M. G.; Read, R. J.; Richardson, J. S.; Richardson, D. C.; Sammito, M. D.; Sobolev, O. V.; Stockwell, D. H.; Terwilliger, T. C.; Urzhumtsev, A. G.; Videau, L. L.; Williams, C. J.; Adams, P. D. Macromolecular Structure Determination Using X-Rays, Neutrons and Electrons: Recent Developments in Phenix. *Acta Crystallogr., Sect. D: Struct. Biol.* **2019**, *75*, 861–877.

(37) Emsley, P.; Lohkamp, B.; Scott, W. G.; Cowtan, K. Features and Development of Coot. *Acta Crystallogr., Sect. D: Biol. Crystallogr.* **2010**, *66*, 486–501.

(38) Pricer, R.; Gestwicki, J. E.; Mapp, A. K. From Fuzzy to Function: The New Frontier of Protein-Protein Interactions. *Acc. Chem. Res.* **2017**, *50*, 584–589.

(39) Morreale, F. E.; Kleine, S.; Leodolter, J.; Junker, S.; Hoi, D. M.; Ovchinnikov, S.; Okun, A.; Kley, J.; Kurzbauer, R.; Junk, L.; Guha, S.; Podlesainski, D.; Kazmaier, U.; Boehmelt, G.; Weinstabl, H.; Rumpel, K.; Schmiedel, V. M.; Hartl, M.; Haselbach, D.; Meinhart, A.; Kaiser, M.; Clausen, T. BacPROTACs Mediate Targeted Protein Degradation in Bacteria. *Cell* **2022**, *185*, 2338.

(40) *Guide for the Care and Use of Laboratory Animals*, 8th ed.; National Academies Press (US): Washington (DC), 2011.